

Attitude control of small unmanned four-rotor helicopter based on adaptive inverse control theory

Li Jin-song*, Cao Xi**

*Eng. Training Center, Shanghai Jiao Tong University, Shanghai 200240, China, E-mail: ljs@sjtu.edu.cn

**School of Electronic Information and Electrical Engineering, Shanghai Jiao Tong University, Shanghai 200240, China, E-mail: cx32167@sjtu.edu.cn

crossref <http://dx.doi.org/10.5755/j01.mech.18.1.1288>

1. Introduction

Small unmanned four-rotor helicopter (four-rotor) is a kind of noncoaxial, multirotor, dished vehicle with vertical take off and landing (VTOL) ability. Due to the complexity, strong coupling and sensitivity effects on the environment of four-rotor's dynamic model, the controller must have high quality of robust and adaptive. According to these requirements, a lot of control theory have been proposed, including Backstepping [1], LQG [2], ADRC [3] and adaptive sliding mode [4]. This paper propose a new method that applying the adaptive inverse control (AIC) theory to attitude stabilization control. The AIC theory uses output difference of real object and its co-input model to drive the inverse model. This model can generate a filtered noise and interference. And the ultimate input is the difference between previous one and this filtered signal.

Sections 2-3 construct the experimental platform hardware and dynamic model of four-rotor; Section 4 conducts the structure of AIC controller; Section 5 gives the final result of applying AIC theory to four-rotor attitude control experimental.

2. Experimental platform hardware system of four-rotor

The experimental platform for four-rotor is shown in Fig. 1.



Fig. 1 Experimental platform for four-rotor

The experimental platform has orthogonal glass-fiber pipes structure, 4 Hi-Model brushless motors and 4 rigid plastic rotors. When the rotors on X-axis rotate clockwise, the other rotors on Y-axis will rotate counterclockwise simultaneously so that the anti-torque can be cancelled out. In the process of flight control,

changing the speed of all rotors equally at the same time will cause the up-and-down motion of the four-rotor. Increasing the speed of one rotor meanwhile equally decreasing the one belongs to the same group (each two rotors on the same axis is called a group), the pitch and rolling motion can be accomplished. In addition, the yaw motion will be generated by increasing the speed of one group while decreasing the speed of the other.

The hardware of this system consists of power unit, inertia measurement unit (IMU), airborne GPS navigation and positioning unit, wireless communication unit, height measurement unit, motor speed measurement unit and embedded microcontroller unit. The detailed devices of each module are shown in Table.

Table

Detailed devices of each module

Module	Devices
IMU	UZZ9001+KMZ41 ENC-03RC LIS302DL(302D)
GPS navigation	Dagama SG-959
Wireless communication	APC802-43
Height measurement	URM05 (ultrasonic)
Rotor speed measurement	Hall sensor A1101
Central processor	ARM7

3. Dynamic model of four-rotor

Two coordinate systems are set up to describe the dynamic model of four-rotor, which are shown in Fig. 2.

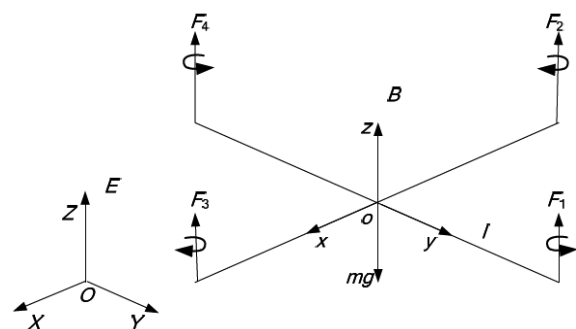


Fig. 2 Earth coordinate system and body coordinate system

$E(X, Y, Z)$ is an absolute ground coordinate system which relates to a stationary reference point. The center of frame, says O , is chosen as the origin. The velocities and displacements of the four-rotor are measured in this system. And the body coordinate system $B(x, y, z)$ is

a system whose origin is the geometric center of four-rotor. The pitch angle θ , roll angle ϕ and travel angle ψ (Euler attitude angles) are described in this system.

According to Newton-Euler equation [5-8], we can get

$$\left. \begin{aligned} m\ddot{x} &= F_x - k_1\dot{x} \\ m\ddot{y} &= F_y - k_1\dot{y} \\ m\ddot{z} &= F_z - k_1\dot{z} \end{aligned} \right\} \quad (1)$$

where m is the mass of model; F_x, F_y, F_z , are the components of the lift force belong to each axis. Air resistance is assumed to be proportional to the speed of model, with a

$$\left. \begin{aligned} \ddot{x} &= \frac{\sin\psi \sin\phi + \cos\psi \sin\theta \cos\phi}{m} (F_1 + F_2 + F_3 + F_4) - k_1\dot{x} \\ \ddot{y} &= \frac{-\cos\psi \sin\phi + \sin\psi \sin\theta \cos\phi}{m} (F_1 + F_2 + F_3 + F_4) - k_1\dot{y} \\ \ddot{z} &= \frac{\cos\theta \cos\phi}{m} (F_1 + F_2 + F_3 + F_4) - k_1\dot{z} - g \end{aligned} \right\} \quad (3)$$

Similarly, the angular velocities p, q, r can be described by Euler angles ψ, ϕ, θ which is shown in Eq. (4)

$$\begin{bmatrix} p \\ q \\ r \end{bmatrix} = \begin{bmatrix} 1 & 0 & -\sin\theta \\ 0 & \cos\phi & \sin\phi \cos\theta \\ 0 & -\sin\phi & \cos\phi \cos\theta \end{bmatrix} \begin{bmatrix} \dot{\phi} \\ \dot{\theta} \\ \dot{\psi} \end{bmatrix} \quad (4)$$

According to Newton-Euler equation, we can get

$$\left. \begin{aligned} I_x \dot{p} &= l(F_4 - F_1) + (I_y - I_z)qr - I_R q(-\omega_1 + \omega_2 - \omega_4 + \omega_3) \\ I_y \dot{q} &= l(F_2 - F_3) + (I_z - I_x)rp + I_R p(-\omega_1 + \omega_2 - \omega_4 + \omega_3) \\ I_z \dot{r} &= M_R + (I_x - I_y)pq = \lambda(F_1 + F_4 - F_2 - F_3) + (I_x - I_y)pq \end{aligned} \right\} \quad (5)$$

where l is the distance from the center of the model to the center of any of the rotors (the action point of lift force); λ is a scale factor between z axis torsional torque and the lift force; I_x, I_y, I_z are the rotating moments of the four-rotor reference to axis x, y, z, respectively. Therefore, $(I_y - I_z)qr, (I_z - I_x)rp, (I_x - I_y)pq$ reflect of the gyroscopic effect of the model; and $-I_R q(-\omega_1 + \omega_2 - \omega_4 + \omega_3), -I_R p(-\omega_1 + \omega_2 - \omega_4 + \omega_3)$ are the gyroscopic effect of the rotors.

In order to take further derivation, some more variables are defined: u_1 is defined as the sum of F_1, F_2, F_3, F_4 ; u_2 is the resultant moment of the rotors which generate the roll angle, while u_3 is the resultant moment of the rotors which generate the pitch angle; finally, u_4 is defined as the travel moment due to adjusting the rotor speed, which is proportional to the lift force. So there is a matrix U

$$U = \begin{bmatrix} u_1 \\ u_2 \\ u_3 \\ u_4 \end{bmatrix} = \begin{bmatrix} 1 & 1 & 1 & 1 \\ 0 & l & 0 & -l \\ -l & 0 & l & 0 \\ -\lambda & \lambda & -\lambda & \lambda \end{bmatrix} \begin{bmatrix} F_3 \\ F_4 \\ F_2 \\ F_1 \end{bmatrix} \quad (6)$$

coefficient k_1 . Therefore, $k_1\dot{x}, k_1\dot{y}, k_1\dot{z}$ is the air resistance which is opposite to the speed vector. Furthermore, there is a relationship as shown in Eq. (2)

$$\begin{bmatrix} F_x \\ F_y \\ F_z \end{bmatrix} = (F_1 + F_2 + F_3 + F_4) A^{BE} \begin{bmatrix} 0 \\ 0 \\ 1 \end{bmatrix} - m \begin{bmatrix} 0 \\ 0 \\ g \end{bmatrix} \quad (2)$$

where F_1, F_2, F_3, F_4 are the lift forces of each rotor, which are proportional to square of rotation speed; A^{BE} is defined as a transfer matrix between body coordinate system and the inertia one. Rearrange Eqs. (1) and (2), the displacement dynamic equation can be described by Eq. (3)

Taking $I_x = I_y$ into consideration and neglecting the gyroscopic effect of the rotors. Rearrange Eqs. (4)-(6), the dynamic equations of the Euler angles can be described by Eq. (7)

$$\left. \begin{aligned} \ddot{\phi} &= \frac{u_2 + \dot{\theta}\dot{\psi}(I_y - I_z)}{I_x} \\ \ddot{\theta} &= \frac{u_3 + \dot{\phi}\dot{\psi}(I_z - I_x)}{I_y} \\ \ddot{\psi} &= \frac{u_4}{I_z} \end{aligned} \right\} \quad (7)$$

Therefore Eqs. (3), (7) are the dynamic equations of the four-rotor.

4. Design of AIC controller

AIC is successfully utilized in many fields [9]-[13], and especially suitable for the control objects having multivariable, nonlinear, strong coupling and interference sensibility. The completed structure of controller is shown in Fig. 3, which was in the published paper of authors [14].

Under the ideal forward and inverse model condition, the unique antiinterference structure can make the transfer function, the ratio of output and the noise from sensors, approach to zero. Which means the noise and interference can be effectively restrained at the output [15, 16]. Due to this characteristic, the AIC theory can be applied to antiinterference and attitude control of four-rotor.

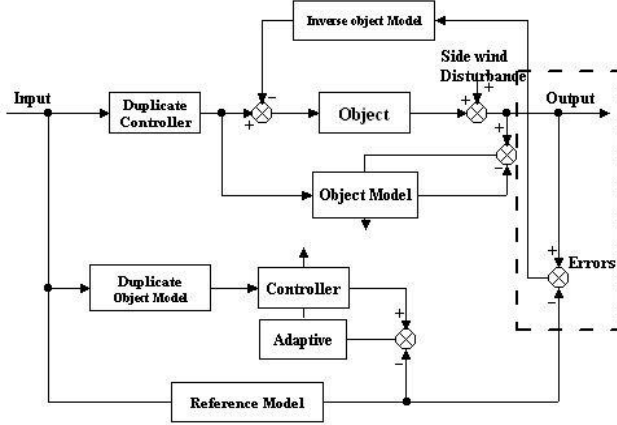


Fig. 3 The completed structure of AIC controller

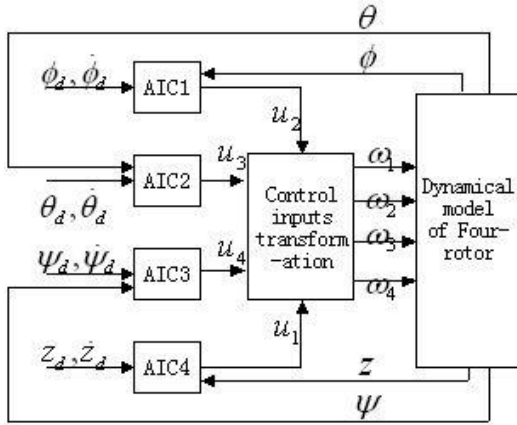


Fig. 4 Four-rotor control system diagram based on AIC

According to the form of the dynamic equations, the flight control of the four-rotor is divided into four independent channels. They are roll angle control channel, pitch angle control channel, travel angle control channel and height control channel. The structure of four-rotor control system based on AIC is shown in Fig. 4.

Where AIC1, AIC2, AIC3, AIC4 is in roll angle, pitch angle, travel angle and height control channel, respectively.

Least mean square (LMS) algorithm is a typical control algorithm of AIC method. Since simulation results show that, for the model presented in this paper, LMS algorithm has a slow convergence rate and easily divergent. Therefore, N-LMS algorithm is used to identify the parameters of the controller and the reference model. The iterative formula is shown in Eq. (8)

$$W_{k+1} = W_k + \mu \frac{e_k X_k}{\gamma + \|X_k\|^2} \quad (8)$$

where X_k, W_k and e_k are the output vector of filter, desired output, weight vector and error; $\gamma > 0$ is a positive, which

is small enough to confirm the step is bounded; $1 > \mu > 0$ is the weight coefficient. Taking the roll angle control channel for example, the iterative formula is

$$\phi_{k+1} = \phi_k + \mu \frac{e_k \phi_k}{\gamma + \|\phi_k\|^2} \quad (9)$$

Similar for the other three models, the rotation speed of the rotors is described by Eq. (10).

The rotation speed of rotors is controlled by processor so that the lift force, further the flight attitude, can be stabilized.

$$\left. \begin{aligned} \omega_1 &= \sqrt{(u_1 - 2u_3 / l) / 4k_1 - u_4 / 4\lambda} \\ \omega_2 &= \sqrt{(u_1 - 2u_2 / l) / 4k_1 + u_4 / 4\lambda} \\ \omega_3 &= \sqrt{(u_1 + 2u_3 / l) / 4k_1 - u_4 / 4\lambda} \\ \omega_4 &= \sqrt{(u_1 + 2u_2 / l) / 4k_1 + u_4 / 4\lambda} \end{aligned} \right\} \quad (10)$$

5. Attitude control experiment of four-rotor

In actual experiment, the length and width of Four-rotor are equal, $L = W = 0.54$ m; height $H = 0.15$ m; $l = 0.24$ m; $m = 0.725$ kg. Sunplus microcontroller SPMC75F2413 is used to generate the PWM to control the brushless motor. The lift force is measured by high-accuracy electronic balance (force sensor).

According to the measurement, the relationship between lift force F and PWM can be described as shown in Eq. (11)

$$PWM = 1105 - 261 \times F + 22.23 \times F^2 \quad (11)$$

Through three-line pendulum, the moment can be calculated by Eq. (12)

$$J = \frac{mga^2}{4\pi^2 b} T^2 \quad (12)$$

where a is the distance from suspension line to body of four-rotor, b is the length of suspension line. And T is the swing period. Therefore, the rotating moment is obtained as

$$I_z = \frac{mga^2}{4\pi^2 b} T_z^2 = 0.0664 \text{ kg m}^2$$

$$I_x = I_y = \frac{mga^2}{4\pi^2 b} T_{xy}^2 = 0.0479 \text{ kg m}^2$$

where $a = 0.512$ m, $b = 1.2$ m, $T_z = 1.33$ s, $T_{xy} = 0.777$ s.

And the relationship of u_i and F_i are described by Eq. (13)

$$\left. \begin{aligned} u_1 &= F_1 + F_2 + F_3 + F_4 \\ u_2 &= (F_4 - F_1) \times l \\ u_3 &= (F_2 - F_3) \times l \\ u_4 &= \lambda (F_1 + F_4 - F_2 - F_3) \end{aligned} \right\} \quad (13)$$

Then combined with Eq. (11), $u_1 \sim u_4$ can be easily calculated. Moreover, using these values ω_i can be obtained by Eq. (10).

Setting $k_1 = 2.703 \times 10^{-4}$. Then, at time 4 s, the rotation speed of the rotors can be calculated as $\omega_1 = 30.7667$ r/s, $\omega_4 = 31.1167$ r/s, $\omega_2 = 30.8167$ r/s, $\omega_3 = 30.8627$ r/s, ($u_4 / 4\lambda = (F_1 + F_4 - F_2 - F_3) / 4$, λ can be divided out so that there is no value set for it).

And the values sampled by Hall sensors are $\omega_1 = 30.6167$ r/s, $\omega_4 = 30.9267$ r/s, $\omega_2 = 30.7447$ r/s, $\omega_3 = 30.8627$ r/s. The errors are in 0.5%, which meet the requirement of the experiment. In this experiment, the average values of these two ω are used as the samples of rotation speed and a desired result was obtained. Since the rotation speed has a great influence on lift force, and the Euler angles. Therefore, the flight attitude control can be accomplished by rotation speed regulation.

The control experiment was conducted on the platform, which was proposed in Section 2. The initial state was: roll angle - 1.3 rad, pitch angle - 1.3 rad and travel angle - 5.2 rad. In the process, all these angles were turned to 0 rad. The stable attitude state of the four-rotor is shown in Fig. 5.



Fig. 5 Platform control experiment

In this experiment, the attitude is measured by IMU. Then, under the control of ARM7, the sampled signals are transmitted to PC through wireless module. After analyzing, the effect of AIC control can be obtained and the input signal can be compensated by the feedback.

6. Conclusions

1. Though the experiment, it can be concluded that the steady-state error of Euler angles, which is caused by the sensor noise can be limited in a small interval by AIC method.

2. It also can show the robust of AIC method. Moreover, AIC is proved to suitable for the control of the four-rotor which has the requirement of stability and rapidity.

References

1. **Bouabdallah, S.; Siegwart, R.** 2005. Backstepping and sliding-mode techniques applied to an indoor micro quadrotor, International Conference on Robotics and Automation, Barcelona, Spain.
2. **Kenzo Nonami; Farid Kendoul; Satoshi Suzuki; et al.** 2010. Autonomous control of a mini quadrotor vehicle using LQG controllers, Autonomous Flying Robots, Part I, 61-76
3. **WANG Jun-sheng; MA Hong-xu; CAI Wen-lan; et al.** 2008. Research on micro quadrotor control based on ADRC, Journal of Projectiles, Rockets, Missiles and Guidance 28(3): 31-34.
4. **Daewon Lee; H. Jin Kim and Shankar Sastry.** 2009. Feedback linearization vs. adaptive sliding mode control for a quadrotor helicopter, International Journal of Control, Automation, and Systems 7(3): 419-428. <http://dx.doi.org/10.1007/s12555-009-0311-8>
5. **Jinhyun Kim; Min-Sung Kang; Sangdeok Park.** 2010. Accurate modeling and robust hovering control for a quad-rotor VTOL aircraft, Journal of Intelligent & Robotic Systems 57(1-4): 9-26. <http://dx.doi.org/10.1007/s10846-009-9369-z>
6. **Metin Tarhan; Erdinç Altug.** 2010. EKF based attitude estimation and stabilization of a quadrotor UAV using vanishing points in catadioptric images, Journal of Intelligent & Robotic Systems, Online First™.
7. **Cowling, Ian D.; Yakimenko, Oleg A.; Whidborne, James F. et al.** 2010. Direct method based control system for an autonomous quadrotor, Journal of Intelligent & Robotic Systems 60(2): 285-316. <http://dx.doi.org/10.1007/s10846-010-9416-9>
8. **Sanchez, L.R.; García Carrillo; Rondon, E. et al.** 2011. Hovering flight improvement of a quad-rotor mini UAV using brushless DC motors, Journal of Intelligent & Robotic Systems 61(1-4): 85-101. <http://dx.doi.org/10.1007/s10846-010-9470-3>
9. **Sadeghi MS; Momeni HR.** 2009. A new impedance and robust adaptive inverse control approach for a teleoperation system with varying time delay, Science in China Series E-Technological Sciences 52(9): 2629-2643.
10. **Yang Zhi-dong; Huang Qi-Tao; Han Jun-Wei; Li Hong-ren.** 2010. Adaptive inverse control of random vibration based on the filtered-X LMS algorithm, Earthquake Engineering and Engineering Vibration 9(1): 141-146. <http://dx.doi.org/10.1007/s11803-010-9011-x>
11. **Dong Zheng-hong; Wang Yuan-qin.** 2007. Application of neural network inverse control system in turbo decoding, Journal of Electronics (China) 24(1): 27-31. <http://dx.doi.org/10.1007/s11767-005-0092-z>
12. **Bao Yan; Wang Hui; Zhang Jing.** 2010. Adaptive inverse control of variable speed wind turbine, Nonlinear Dynamics 61(4): 819-827. <http://dx.doi.org/10.1007/s11071-010-9689-3>
13. **Sahraei B. Ranjbar; Nemati, A.; Safavi, A.A.** 2010. Real-time parameter identification for highly coupled nonlinear systems using adaptive particle swarm optimization, Mechanika 6(86): 43-49.
14. **LI Jin-song; CAO Xi; YAN Guo-zheng and SONG Li-bo.** 2010. Hovering control of unmanned small size helicopter based on adaptive inverse control theory, International Conference on Digital Manufacturing and Automation 1: 804-810.
15. **Pang Chee-khiang; Tam Sai-cheong; Guo Guo-xiao; et al.** 2009. Improved disturbance rejection with online adaptive pole-zero compensation on a Φ -shaped PZT

active suspension, *Microsyst. Technology* 15: 1499-1508. <http://dx.doi.org/10.1007/s00542-009-0796-3>

16. **Li Chun-hua; Zhu Xin-jian; Sui Sheng; et al.** 2009. Adaptive inverse control of air supply flow for proton exchange membrane fuel cell systems, *Journal of Shanghai University (English Edition)* 13(6): 474-480. <http://dx.doi.org/10.1007/s11741-009-0610-3>

Li Jin-song, Cao Xi

KETURIŲ ROTORIŲ MAŽO BEPILOČIO
SRAIGTASPARNIO PADĖTIES KONTROLĖ
REMIANTIS ADAPTYVIAJA INVERSINE
KONTROLĖS TEORIJA

Re z i u m ė

Straipsnyje pasiūlytas keturių rotorių mažo bepiločio sraigtasparnio dinaminis modelis, sukurtas remiantis Niutono ir Eulerio teorija. Adaptyvi inversinė kontrolės (AIC) teorija pirmą kartą buvo panaudota mažo bepiločio keturių rotorių sraigtasparnio kontrolei, o padėties stabilizavimo kontrolė pritaikyta eksperimentinei platformai. Eksperimentas parodė, kad AIC tinka mažų bepiločių keturių rotorių sraigtasparnių padėčiai valdyti.

Li Jin-song, Cao Xi

ATTITUDE CONTROL OF SMALL UNMANNED
FOUR-ROTOR HELICOPTER BASED ON ADAPTIVE
INVERSE CONTROL THEORY

S u m m a r y

A dynamic model of small unmanned four-rotor built according to Newton-Euler formalism was proposed in this paper. Base on this model, Adaptive Inverse Control (AIC) Theory was used in the control of the small unmanned four-rotor for the first time and the attitude stabilization control was also realized on the experimental platform. The attitude control experiment indicates that AIC is robust in the attitude control of the small unmanned four-rotor.

Keywords: attitude control, small unmanned four-rotor helicopter, adaptive inverse control theory.

Received March 23, 2011

Accepted February 02, 2012